Numerical simulation of soil curling during desiccation process

K.M. Tran, H.H. Bui, J. Kodikara
MCG Lab, Department of Civil Engineering, Monash University, Melbourne, Australia
M. Sánchez
Zachry Department of Civil Engineering – Texas A&M University

ABSTRACT: Curling is a common phenomenon occurring in nature soils due to the rearrangement of soil particles during the desiccation process. The occurrence of curling in soils is generally associated with desiccation cracking, which can cause significant damages to geo-infrastructures such as slopes, embankments and pavements. Therefore, understanding the mechanisms of soil curling is vital to deal with key issues, which are relevant to many applications in geotechnical engineering. In this paper, experimental and numerical studies are conducted to provide insights into mechanisms of soil curling induced by moisture evaporations. The discrete element method (DEM) with a new water particle concept is proposed to facilitate the modelling of process, while an artificial clay made of kaolin is adopted in the experiment. Experimental results show that the drying process is separated into three stages: a constant evaporation rate stage, a falling evaporation rate stage and an equilibrium evaporation rate stage. The upward curling is initiated even when the specimen stage is close to the liquid limit stage. Comparison between experiments and simulations suggested that the proposed modelling approach can capture the initiation and development of the upward curling in clay soils, and it is a promising approach to studying soil curling phenomenon.

1 INTRODUCTION

In nature, under climate changes such as an increase in temperature and decrease in relative humidity, soils may lose its moisture content. Consequently, liquid bridges start to form between soil particles and capillary pressure or capillary force develops. The force draws soil particles toward each other and the soil layer shrinks. This process is called desiccation. In expansive clay, this process is severe. It may cause the occurrence of cracks, and the development of the soil curling (Konrad & Ayad, 1997). The study of Berney et al. (2008) demonstrated that occurrence of curling in soils generally enhances the development of desiccation cracking process. Therefore, understanding the mechanism of soil curling is vital to deal with key issues which are relevant to many applications in geotechnical engineering.

Over the past decades, there have been substantial research work directed at studying soil curling and its associated desiccation cracking mechanisms using field observations (Kindle, 1923; Allen, 1986), traditional laboratory testing techniques (Kindle, 1917; Bradley, 1933; Kodikara et al., 2004) or advanced 3D scanner (Zielinski et al., 2014). These studies have revealed that soil curling can be upwards or downwards depending on various factors such as the grain size distribution in vertical direction (Bradley, 1933; Allen, 1986; Zielinski et al., 2014); drying conditions (Bradley, 1933); salt existence and concentration (Kindle, 1923; Kindle, 1926; Bradley, 1933), and clay content (Kindle, 1917). It has been explained that as the drying rate is different along the height of soil specimen, the shrinkage stress profile is non-uniform, causing bending moments to increase and thus lifting the edge of the specimen off to form the concave curling, or lifting off the specimen at the middle to form the convex curling. This concept was verified in continuum-based numerical study (Kodikara et al., 2004). The soil curling behavior can also be explained as the existence of capillary force. The vertical component of capillary forces of the particles which are near edges is smaller than that of other particles, so the settlement of those particles are different and it causes initial concave curling (Zielinski et al., 2014). However, how the sample is lifted off remains elusive. Therefore, further studies on mechanism of soil curling are necessary.

So far, continuum and dis-continuum approaches have been applied to study many aspects of soils and rock behavior (Bui et al., 2014; Bui et al., 2015

Nguyen et al., 2016a; Nguyen et al., 2016b, Gui et al., 2016a, Nguyen et al., 2017, Tran et al., 2017) and dis-continuum approach in general or discrete element method (DEM) in particular is very powerful as both macro and micro views can be investigated (Lee et al., 2012; Tran et al., 2012; O'Sullivan, 2014). In the area of soil desiccation, discrete element method (DEM) has been utilized to study soil desiccation cracking in both two and three dimensions (Peron et al, 2009; Sima et al., 2014; Gui et al., 2016b). These studies demonstrate that DEM could capture well crack initiation and development in clay soils. Furthermore, the effect of the thickness on the cracking network could be well captured. Accordingly, DEM is utilized to study the soil curling process in this study.

In this paper, both experimental and numerical studies are conducted to investigate mechanisms underpinning the soil curling phenomenon. First, the experimental procedure and results are discussed. Then, the simulation approach using the proposed discrete element model is described. Finally, the proposed approach is employed to study the curling behavior of rectangular slurry soil samples undergoing drying process and numerical results are compared to those of experiments.

2 EXPERIMENTAL STUDY

2.1 *Experiment procedure*

The soil sample is prepared by thoroughly mixing pure kaolin NY clay with properties listed in Table 1 with distilled water at 1.35 times liquid limits to form a slurry clay mixture. The mixture is then poured into a Perspex mould with 250mm long, 25mm wide and 12.5mm deep. To eliminate restraints of soil particles movements on the boundaries, all inner sides including the base wall of the mould are greased prior to pouring the slurry soil. The specimen is vibrated for five minutes by using a vibration device to remove entrapped air bubbles and its surface is flattened by using a spatula. Next, the prepared specimen is covered with plastic membrane and left in a desiccator for around 24 hours to allow the soil sample to hydrate uniformly. Finally, the soil sample is placed on a weighing balance with 0.001g accuracy and is dried under a 500W lamp with 75mm length bulb, 180mm diameter lampshade, and 1000mm lamp distance. A camera (Nikon D5100) is set up to take pictures of the long side face of the sample. During the drying process, the weighing balance and camera are recorded every 15 minutes. In addition, a sensor is placed close to the specimen to continuously measure temperature and relative humidity of the soil specimen. The temperature and humidity during the test were fairly constant, around 28^0C±1^0C, and 25%±3%.

Table 1. Soil properties (Shannon, 2013).

Index property	
Liquid limit, LL(%)	54.8
Plastic limit, PL (%)	26
Plasticity Index, PI (%)	28.8
Linear shrinkage (%)	6.9
Specific gravity	2.62
Soil classification	CH

2.2 *Experiment results*

The water content of the specimen during the drying period is presented in Figure 1. It can be observed that the drying process can be separated into three stages: a constant evaporation rate stage, a falling evaporation rate stage, and an equilibrium evaporation rate stage. During the constant evaporation rate stage, the water content decreases linearly with drying time until it reaches 10.2%. After this point, the drying process moves into a falling evaporation rate stage, in which the rate of change of the water content is slowed down until 2.2% and remains around this value afterward (equilibrium evaporation rate stage). The evolution of water content of the sample under drying agrees well with findings of previous studies for other types of clay (Tang et al., 2011).

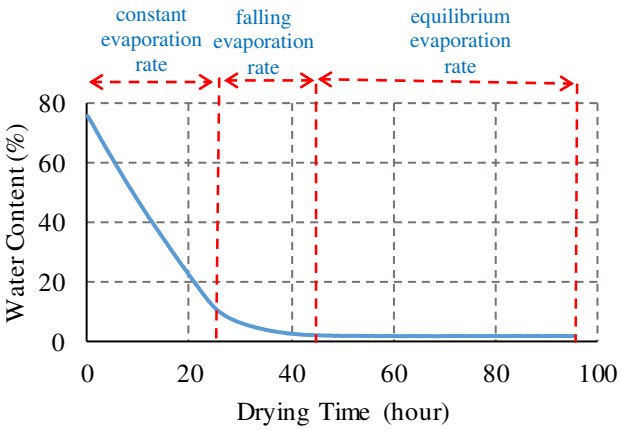

Figure 1. Water content of the specimen during drying process.

The shrinkage process of the kaolin clay sample is presented in Figure 2. It can be observed that, as time goes on, water evaporation causes the water content of soil sample to decrease, leading to the shrinkage of the soil sample in all directions. Initially, the shrinkage in vertical direction is more dominant. The specimen then moves off the right and left sides of the mould after 4.25 hours and 5 hours, respectively, and the shrinkage along the longest side

of the specimen dominates the shrinkage process. The soil shrinkage is negligible when the water content of the specimen is 27.52%, even though water still evaporates as illustrated by the decrease in the water content from 27.52% to 1.94% (Figure 2). The upward curling can be observed at the edges of the samples after drying the specimen about 11 hours, becomes clearer after 17.75 hours and stops developing after this time. The upward curling initiates when the water content of the specimen is 44.34%, which is close to liquid limit of the kaolin NY clay. In other words, the curling takes place even when the specimen is still saturated. This phenomenon is the same as the first development of a crack in slurry clay.

It is noted that because the overall length of the bulb and lampshade adopted in the experiment were slightly shorter than that of the sample, the temperature distribution on the surface of the specimen might be lightly non-uniform. This might contribute to the delay in detaching of the left side of the specimen, the non-uniform settlement along the sample and the minor difference in lift-off height of the edges.

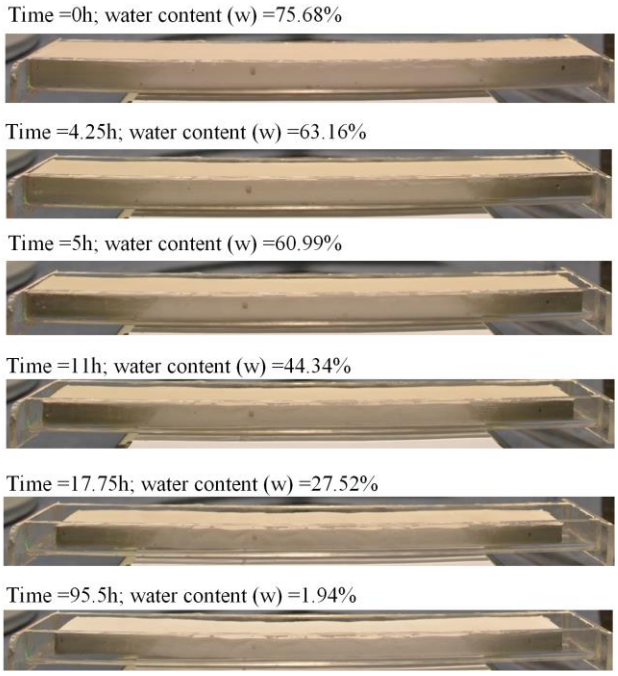

Figure 2. Shrinkage process of the kaolin clay sample.

3 NUMERICAL STUDY

3.1 *Modelling concepts and sample preparation*

In slurry clayey soil samples, clayey particles interact each other by inter-particle forces including van deer Waal force, double layer force, born's repulsive force. These forces help particles to suspend in water and form the slurry state. To reassemble a similar clay system in DEM simulations, this research proposes to adopt the water particle concept in the DEM simulation as shown in Figure 3 (Tran et al., 2018). The main idea of the proposed approach is to use another set of particles, namely "*water particles*", to represent the water volume in a slurry clay specimen, while clay particles are used to represent the solid phase in the specimen. The water particles must be generated in such a way to avoid any direct contact between solid particles. The water particles are chosen randomly within a certain range of radius, which is much smaller than that of clay particles, to fill gaps among clay particles as much as possible. The number of water particles is computed to satisfy the initial water content of the experiment. During the sample preparation process, it is important to ensure clay and water particles "touch" each other without overlapping to eliminate stress-locking affects. All water particles have no friction and interact with each other and other soil particles via the spring model (Tran et al., 2018).

As around 80% of clay particles ranges from 1μ to 3μ (Shannon, 2013), to reduce computation time due to very small size of particles, uniform particle distribution ranging from 1mm to 3mm is used in this study to represent clay particles, while another set of uniformly distributed particles ranging from 0.8mm to 1.2mm is adopted for water particles. The chosen numbers of clay particles satisfy the water content of the experiment. In addition, in DEM simulations, the drying process is simulated from water content of 46.5% which is lower than the liquid limit the initial water content of the experiment (liquid limit = 54.8%, water content of experiment = 75.68%). The stiffness k_n and k_s for the soil and water particles are $1x10^7$ and $5x10^6$, respectively. The friction coefficient between soil particles is chosen to be 0.5, while that of water particles and wall boundary is 0.

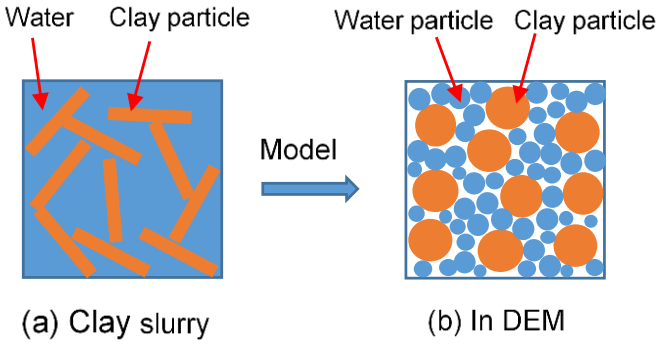

Figure 3. Water particle concept (Tran et al., 2018).

3.2 *Drying process*

The drying process of the slurry clay sample is simulated by reducing the size of water particles. In particular, the radius of water particles with respect to time (t) can be computed using an empirical model

proposed by Peron et al. (2009) for dual particles, consisting of both solid and water phases, as equation (1). By using this equation, the radius of particles which are close to the top edge of the specimen decreases faster. In other word, the evaporation rate is faster on the top of the specimen.

$$R_w = R_{w0} e^{((-\alpha_1(1-\frac{z}{z_0})-\alpha_2\frac{z}{z_0})\frac{t}{\tau})} \quad (1)$$

where R_{w0} and R_w are the radius of the water particles at time t = 0 and t, respectively; α_1 and α_2 (α_1/α_2=0.5) are shrinkage parameters, which is calculated from experimental water contents; τ is the total duration of the experiment; z is the vertical coordinate of the water particle, and z0 is the reference height.

As water evaporates during the drying process, suction inside the specimen increases. To capture the effects of changes in soil suction on soil particles, a liquid bridge force model (Lambert et al., 2008) can be adopted as follows:

$$F_{cw} = -n\frac{2\pi R\gamma\cos\theta}{1+(H/2d_{sp})} \quad (2)$$

with

$$d_{sp} = \frac{H}{2}(-1+\sqrt{1+2V_{lb}/(\pi RH^2)}) \quad (3)$$

$$R = \frac{2R_iR_j}{R_i+R_j} \quad (4)$$

where V_{lb} is the volume of the liquid bridge; θ is the contact angle; γ is the surface tension of water; H is the distance from surface to surface of two spheres; R_i and R_j are the diameter of spheres i and j, respectively; and n is an amplifying factor ($n = r^{(m)}/r^{(p)}$ with $r^{(m)}$ and $r^{(p)}$ being the radii of particles used in simulation and real particles; in this study n=1000) (Jiang et al., 2004).

As could be seen from equation (3), the volume of liquid bridge is required to calculate the capilarry force. However, it is difficult or imposible to estimate this parameter during the drying process. To faciliate the calculation procedure, the following equation is proposed by introducing a variable *f(w)* which is a function of water content into equation (3) as follows:

$$F_{cw}^{DEM} = -f(w)n\frac{2\pi R\gamma\cos\theta}{1+(H/2d_{sp})} \quad (5)$$

By using equation (5), the volume of the liquid bridge is the same for every pair of particles and does not change during the drying process. Nevertheless, the water content function *f(w)* is required and can be calculated through a curve fitting procedure by mapping the soil suction computed from the DEM analysis of a representative volume element (RVE) to that of experimental data (i.e. the soil water characteristic curves). According to Scholtès et al. (2009), the net stress of a RVE consisting of clay and water particles is defined as follows:

$$\sigma_{ij}^{net} = \sigma'_{ij} + \sigma_{ij}^{cap} \quad (6)$$

where σ_{ij}^{net} is the net stress; σ'_{ij} is the effective stress; and σ_{ij}^{cap} is the capillary stress, which can be computed by:

$$\sigma_{ij}^{cap} = \frac{1}{V}\sum_c F_{i,c}^{cap} x_j^{p,q} \quad (7)$$

where V is the volume of the RVE; F^{cap} is the capillary force at the contact c; and $x^{p,q}$ is the vector pointing from the particle p to the particle q of the contact c.

In addition, as suggested by Houlsby (1997), the net stress can be also defined by:

$$\sigma_{ij}^{net} = \sigma'_{ij} - S_r\psi\delta_{ij} \quad (8)$$

where ψ is the suction; S_r is the degree of saturation; and δ_{ij} is the Kronecker Delta.

By comparing equations (6) and (8), the suction can be calculated using the following equation:

$$\psi = -\frac{1}{3S_rV}\sum_c F_{i,c}^{cap} x_j^{p,q} \quad (9)$$

Equation (9) provides a mean to calibrate the water content function *f(w)* for the calculation of capillary force for a given soil in DEM. The details of this calibration procedure is explained in the next section.

3.3 *DEM calibrations*

To calibrate parameters for DEM simulations, a slurry clay RVE sample of 25mm long, 25mm wide and 25mm deep (Figure 4) is simulated. The specimen preparation process follows the same procedure described in *Section 3.1.* In the simulation, the drying process is conducted to obtain multiple designated water contents. The suction (ψ) at the corresponding water content is then measured within a spherical volume, which has a diameter of 18mm and is located at the center of the specimen. The computed suctions at multiple designated water contents are finally benchmarked against the soil water characteristic curve obtained from experiment to ob-

tain the water content function for DEM simulations. For further details of this calibration process and relevant DEM parameters, we refer readers to Tran et al. (2018). As could be seen from Figure 5, the calibrated water content function provides a very good agreement between the DEM simulation and experiment (Shannon, 2013). This suggests that the proposed approach could be used to simulate the slurry Kaolin NY.

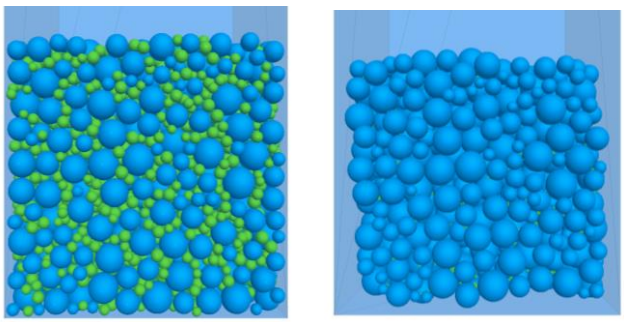

Figure 4. Model setup for calibration f(w): before drying and after drying (blue particles are soil particles; green particles are water particles; 3D view).

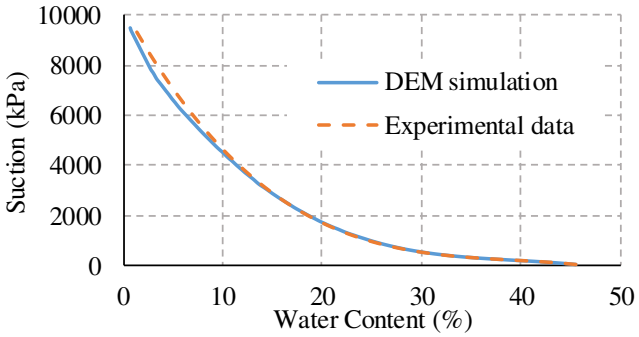

Figure 5. Soil water characteristic curves from the simulation and the experiment.

3.4 *Soil curling simulation*

The soil curling experiment can be now simulated using the calibrated water content function for the slurry Kaolin NY. The size of numerical specimen is the same to that of the curling experiment except that the sample width is now reduced to 15mm to save the computational cost. The same DEM model parameters are adopted in the current simulation and the drying process is also reproduced by reducing the radius of water particles.

Figure 6 shows the curling process of the numerical sample at different water content levels. It can be observed that the upward curling is initiated at the edges of the sample when the water content is 44.4%, which is very close to that of the experiment (see Figure 2 at Time = 11h). Next, the curling continuously develops until reaching its max elevation at the water content of around 11.4%. After this stage, the curled edge starts retreating downwards to its initial position, even though the sample still shrinks during this period. The finding in the current DEM simulation is similar with that of Zielinski et al. (2014) who conducted 2D laser scanner to monitor the development of cracks and curling trend of a disk soil sample. Compared to the experiment on the slurry Kaolin NY (Figure 2), the shrinkage process of the numerical sample in DEM simulation agrees quite well with that observed in the experiment. However, the simulation over-predicts the lift-off height of the curled edges and this can be attributed to the large size of soil and water particles adopted in the current DEM simulation and spherical shape is used instead off flat sheet. Furthermore, the difference in sample width and buck density of the numerical sample can also influences the numerical results and further researches are required to clarify this mechanism.

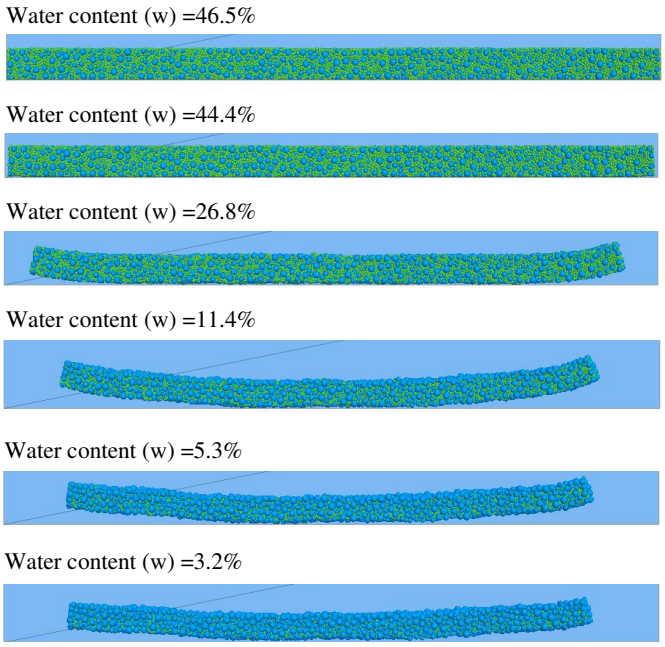

Figure 6. Shrinkage process of the simulation (blue particles are soil particles; green particles are water particles; 2D view).

4 CONCLUSIONS

In this paper, the mechanism of soil curling during desiccation process is studied by experiments and numerical simulations. The experimental drying test is conducted on a slurry kaolin NY clay sample, while the numerical study is carried out the DEM simulation with the proposed water particle concept. The study shows that, under the drying process, the soil specimen continuously shrinks in all directions. Nevertheless, the vertical deformation is more dominant than the horizontal deformation during the initial stage of the drying process, and this behavior is

reverted after a certain time of drying. In addition, the edges of the specimen are lifted up even when the water content of the sample is close to the liquid limit. The curling edges progressively develop to reach its maximum elevation and then retreat downwards to the stable position. The simulation study shows that by adopting the water particle concept, the curling process of the clayey soil can be captured. It proves that the proposed concept is capable of representing physical behavior of soil curling and thus can be applied to provide further insights into soil curling mechanisms.

5 ACKNOWLEDGEMENTS

Funding support from the Australian Research Council via projects DP160100775 (Ha H. Bui, J. Kodikara and M. Sanchez) is gratefully acknowledged.

6 REFERENCES

Allen, J.R.L. 1986. On the curl of desiccation polygons. *Sedimentary Geology* 46: 23–31.

Berney, E.S., Hodo, W.D., Peters, J.F., Myers, T.E., Olsen, R.S., & Sharp, M.K. 2008. Assessment of the effectiveness of clay soil covers as engineered barriers in waste disposal facilities with emphasis on modeling cracking behavior. Tech. Rep. Erdc Tr-08-7. *US Army Corps of Engineers, Engineer Research and Development Center*.

Bui, H.H., Kodikara, J.K., Bouazza, A., Haque, A., & Ranjith, P.G. 2014. A novel computational approach for large deformation and post-failure analyses of segmental retaining wall systems. *International Journal for Numerical and Analytical Methods in Geomechanics* 38(13): 1321-1340.

Bui, H.H., Nguyen, G.D., Kodikara, J.K., & Sanchez, M. 2015. Soil cracking modelling using the mesh-free SPH method. *Australian New Zealand Geomechanics Conference*: 122-129.

Bradley, W.H. 1933. Factors that determine the curvature of mud-cracked layers. *American Journal of Science* 26(5): 55–71.

Gui, Y.L., Bui, H.H., Kodikara, J., Zhang, Qian-Bing., Zhao, J., & Rabczuk, T. 2016. Modelling the dynamic failure of brittle rocks using a hybrid continuum-discrete element method with a mixed-mode cohesive fracture model. *International Journal of Impact Engineering* 87: 146-155.

Gui, Y.L., Zhao, Z.Y., Kodikara, J., Bui, H.H., & Yang, S.Q. 2016b. Numerical modelling of laboratory soil desiccation cracking using UDEC with a mix-mode cohesive fracture model. *Engineering Geology* 202: 14-23.

Houlsby, G. T. 1997. The work input to an unsaturated granular material. *Géotechnique* 47(1): 193–196.

Jiang, M.J., S. Leroueil, & J.M. Konrad. 2004. Insight into shear strength functions of unsaturated granulates by DEM analyses. *Computers and Geotechnics* 31(6): 473-489.

Kindle, E.M. 1917. Some factors affecting the development of mud-cracks. *The Journal of Geology* 25(2): 135–144.

Kindle, E.M. 1923. Notes on mud crack and ripple mark in recent calcareous sediments. *The Journal of Geology* 31(2): 138–145.

Kindle, E.M. 1926. Contrasted types of mud-cracks. *Proceedings and transactions of the Royal Society of Canada* 20(3): 71–75.

Konrad, J.-M., & Ayad, R. 1997. Desiccation of a sensitive clay: field experimental observations. *Canadian Geotechnical Journal* 34: 929–942.

Kodikara, J.K., Nahlawi, H., & Bouazza, A. 2004. Modelling of curling in desiccating clay. *Canadian Geotechnical Journal* 41 (3): 560–566.

Lambert, P., Chau, A., & Delchambre., A. 2008. Comparison between Two Capillary Forces Models. *Langmuir* 24(7): 3157-3163.

Lee., Jong-Sub., Tran, M. K., & Lee, Changho. 2012. Evolution of layered physical properties in soluble mixture: Experimental and numerical approaches. *Engineering geology* 143: 37-42.

Nguyen, G.D., Nguyen, C.T., Bui, H.H., & Nguyen., V. P. 2016a. Constitutive modelling of compaction localization in porous sandstones. *International Journal of Rock Mechanics and Mining Sciences* 83: 57-72.

Nguyen, G.D., Nguyen, C.T., Nguyen., V. P., Bui, H.H., & Shen, L. 2016b. A size-dependent constitutive modelling framework for localized failure analysis. *Computational Mechanics* 58(2): 257-280.

Nguyen, N.H.T., Bui, H.H., Nguyen, G.D., & Kodikara, J. 2017. A cohesive damage-plasticity model for DEM and its application for numerical investigation of soft rock fracture properties. *International Journal of Plasticity* 98: 175-196.

O'Sullivan, C. 2014. Particulate Discrete Element Modelling: A Geomechanics Perspective. *CRC Press*.

Peron, H., et al. 2009. Discrete element modelling of drying shrinkage and cracking of soils. *Computers and Geotechnics* 36(1–2): 61-69.

Scholtès, L., Hicher, P., Nicot, F., Chareyre, B. & Darve, F. 2009. On the capillary stress tensor in wet granular materials. *International Journal for Numerical and Analytical Methods in Geomechanics* 33(10): 1289–1313.

Shannon, B.M. 2013. Fracture Propagation of cohesive soils under tensile loading and desiccation. *Ph.D thesis*. Monash University.

Sima, J., M. Jiang, & C. Zhou. 2014. Numerical simulation of desiccation cracking in a thin clay layer using 3D discrete element modeling. *Computers and Geotechnics* 56: 168-180.

Tang, Chao-Sheng., Bin Shi, Chun Liu, Wen-Bin Suo, & Lei Gao. 2011. Experimental characterization of shrinkage and desiccation cracking in thin clay layer. *Applied Clay Science* 52(1–2): 69-77.

Tran, H.T., Bui, H.H., Nguyen, G.D., & Kodikara, J. 2017. A continuum based approach to modelling tensile cracks in soils. *Sixth Biot Conference on Poromechanics*: 337-344.

Tran, M. K., Shin, Hosung., Byun, Yong-Hoon., & Lee, Jong-Sub. 2011. Mineral dissolution effects on mechanical strength. *Engineering geology* 125: 26-34.

Tran, M. K., Bui, H.H., Kodikara, J.K., & Sanchez, M. 2018. A new DEM approach to model desiccation induced shrinkage curling in slurry soils *(in preparation).*

Zielinski, M., Sanchez, M., Romero, E., & Atique, A. 2014. Precise observation of soil surface curling. *Geoderma* 226-227: 85-93.